

Structured Light Based Depth Edge Detection for Object Shape Recovery

Cheolhwon Kim[†] Jiyoun Park[†] Juneho Yi[†]

Matthew Turk[‡]

[†]School of Information and Communication Engineering
Sungkyunkwan University, Korea
Biometrics Engineering Research Center
{ani4one, jiyp, jhyi}@ece.skku.ac.kr

[‡]Computer Science Department
University of California
Santa Barbara, CA 93106
mturk@cs.ucsb.edu

Abstract

This research features a novel approach that efficiently detects depth edges in real world scenes. Depth edges play a very important role in many computer vision problems because they represent object contours. We strategically project structured light and exploit distortion of light pattern in the structured light image along depth discontinuities to reliably detect depth edges. Distortion along depth discontinuities may not occur or be large enough to detect depending on the distance from the camera or projector. For practical application of the proposed approach, we have presented methods that guarantee the occurrence of the distortion along depth discontinuities for a continuous range of object location. Experimental results show that the proposed method accurately detect depth edges of human hand and body shapes as well as general objects.

1. Introduction

Object contour is valuable information in image analysis problems such as object recognition and tracking. Object contours can be represented by depth discontinuities (aka depth edges). However, the use of traditional Canny edges cannot distinguish between texture edges and depth edges. We describe a structured light based framework for reliably capturing depth edges in real world scenes without dense 3D reconstruction.

1.1. Overview of our approach

The goal of this research is to produce a depth edge map of the real world scene. We have illustrated in Figure 1 the basic idea that detects depth edges. First, as can be seen in Figure 1 (a), we project a white light and structured light consecutively onto a scene where depth edges are to be detected. The structured light

contains a special light pattern. In this work, we have used simple black and white horizontal stripes of equal width. Vertical stripes can be used with the same analysis applied to horizontal stripes. We capture the white light image and the structured light image. Second, we extract horizontal patterns simply by differencing the white light and structured light images. We call this difference image the ‘patterned image’. Refer to Figure 1 (b). Third, we identify depth edges in the patterned image guided by edge information from the white light image. We exploit distortion of light pattern in the structured light image along depth edges. Since the horizontal pattern can be considered a periodic signal with specific frequency, we can easily detect candidate locations for depth edges by applying a Gabor filter to the patterned image [11]. The amplitude response of the Gabor filter is very low where distortion of light pattern occurs. Figure 1 (c) illustrates this process. Finally, we accurately locate depth edges using edge information from the white light image, yielding a final depth edge map as in Figure 1 (d).

However, distortion along depth discontinuities may not occur or be sufficient to detect depending on the distance from the camera or projector. For practical application of the proposed approach, it is essential to have a solution that guarantees the occurrence of the distortion along depth discontinuities irrespective of object location. Figure 2 shows an example situation. Along the depth edges between objects A and B, C and D, the distortion of pattern almost disappears. This makes it not feasible to detect these depth edges using a Gabor filter.

We propose methods to guarantee the occurrence of the distortion for a continuous range of object location. Based on a modeled imaging geometry of camera, projector, object, and its mathematical analysis, we first compute the exact ranges of object location where detection of distortion is not feasible.

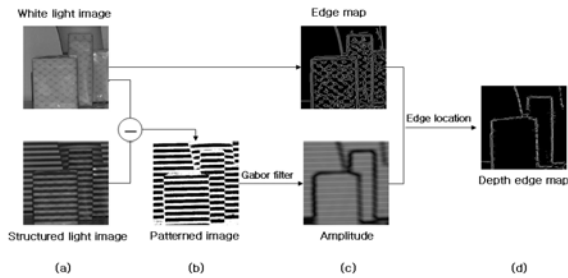


Figure 1. Illustration of the basic idea to compute a depth edge map: (a) capture of a white light image and structured light image, (b) patterned image, (c) detection of depth edges by applying a Gabor filter to the patterned image with edge information from the white light image, (d) final depth edge map

We present two methods that extend the range where detection of the distortion is guaranteed. The first method is based on a single camera and projector setup that simply uses several structural light images with different width of horizontal stripes. The other method exploits an additional camera or projector with the first method. We have used a general purpose LCD projector, however, an infrared projector can be employed with the same analysis in order to apply the method to humans. Experimental results have confirmed that the proposed methods work very well for shapes of human hands and bodies as well as for general objects.

1.2. Related work

Depth edges directly represent shape features that are valuable information in computer vision [2-5]. Unfortunately, few research results have been reported that provide only depth discontinuities without computing 3D information at every pixel in the input image of a scene. On the other hand, most effort has been devoted to stereo vision problems in order to obtain depth information. In fact, stereo methods for 3D reconstruction fail in textureless regions and along occluding edges with low intensity variation [6, 7]. Recently, the use of structured light was reported to compute 3D coordinates at every pixel in the input image [8, 9]. However, the fact that this approach needs a number of structured light images makes it hard to be applicable in realtime.

One notable technique was reported recently for non-photorealistic rendering [10]. They capture a sequence of images in which different light sources illuminate the scene from various positions. Then they use shadows in each image to assemble a depth edge map. This technique was applied to finger spelling recognition [11]. Although very attractive, it only

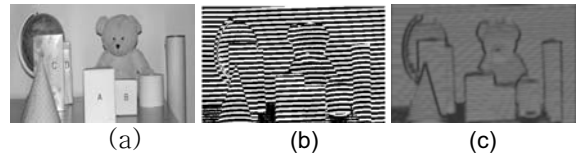


Figure 2. Problem of disappearance of distortion along depth edges depending on the distance of an object from the camera and projector: (a) white light image (b) patterned image (c) amplitude response of Gabor filter applied to the patterned image. Along the depth edges between objects A and B, C and D, in the patterned image (b), the distortion of pattern almost disappears. This makes it infeasible to detect these depth edges using a Gabor filter.

works where shadows can be reliably created. In contrast, our method is shadow free. In addition, by a slight modification of the imaging system so that it can capture white and structured images at the same time, it can be easily applied to dynamic scenes where the camera moves.

The remaining of this paper is organized as follows. In section 2, we describe the application of Gabor filter to detect depth edges in a patterned image. Section 3 presents our methods that guarantee the occurrence of the distortion along depth discontinuities for a continuous range of object location. We report our experimental results in section 4. Finally, conclusions and future work are discussed in section 5.

2. Detecting depth edges

We detect depth edges by projecting structured light onto a scene and exploit distortion of light pattern in the structured light image along depth discontinuities. In order to exploit distortion of light pattern, we use 2D Gabor filtering that is known to be useful in segregating textural regions [1, 12]. We first find candidate depth edges by applying a Gabor filter to the patterned image. We then accurately locate depth edges using edge information from white light image.

2.1. The use of Gabor filter

Since a horizontal pattern can be considered a spatially periodic signal with specific frequency, we can easily detect candidate locations for depth edges by applying a Gabor filter to the patterned image. A 2-D Gabor filter is an oriented complex sinusoidal grating modulated by a 2-D Gaussian function, which is given by

$$G_{\sigma, \phi, \theta}(x, y) = g_{\sigma}(x, y) \cdot \exp[2\pi j \phi(x \cos \theta + y \sin \theta)] \quad (1)$$

where

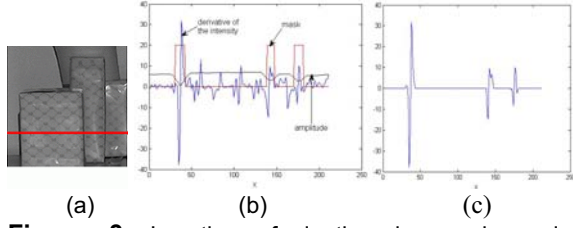


Figure 3. Location of depth edges using edge information from the white light image. (a) white light image, (b) referring to edges in the white light image, (c) location of depth edges

$$g_{\sigma} = \frac{1}{2\pi\sigma^2} \exp\left[-\frac{(x^2 + y^2)}{2\sigma^2}\right]$$

The frequency of the span-limited sinusoidal grating is given by ϕ and its orientation is specified as θ . $g_{\sigma}(x, y)$ is the Gaussian function with scale parameter σ . Decomposing $G_{\sigma, \phi, \theta}(x, y)$ into real and imaginary parts gives

$$G_{\sigma, \phi, \theta}(x, y) = R_{\sigma, \phi, \theta}(x, y) + jI_{\sigma, \phi, \theta}(x, y) \quad (2)$$

where

$$R_{\sigma, \phi, \theta}(x, y) = g_{\sigma}(x, y) \cdot \cos[2\pi\phi(x \cos\theta + y \sin\theta)]$$

$$I_{\sigma, \phi, \theta}(x, y) = g_{\sigma}(x, y) \cdot \sin[2\pi\phi(x \cos\theta + y \sin\theta)].$$

The Gabor filtered output of an image $f(x, y)$ is obtained by the convolution of the image with the Gabor function $G_{\sigma, \phi, \theta}(x, y)$. Thus, its amplitude response can be computed as follows:

$$E_{\sigma, \phi, \theta}(x, y) = \sqrt{[R_{\sigma, \phi, \theta}(x, y) * f(x, y)]^2 + [I_{\sigma, \phi, \theta}(x, y) * f(x, y)]^2}. \quad (3)$$

2.2 Referring to edges in white light image

It is possible to accurately locate depth edges by combining the Gabor filter output and edge information from the white light image. In this work we have used a first derivative technique to detect edges in the white light image but other methods can also be applied. Figure 3 illustrates detection of depth edges. Figure 3 (b) represents the first derivative of the intensity along the line in the white light image in Figure 3 (a). The derivative is then filtered with the mask based on the Gabor amplitude. The amplitude response of an appropriately tuned Gabor filter is also shown. As expected, the amplitude response has low value at the depth discontinuities. The accurate location of depth edges are obtained by finding zero crossing points of the derivative output where the Gabor amplitude is low. See Figure 3 (c). Using this method, we can accurately locate depth edges.

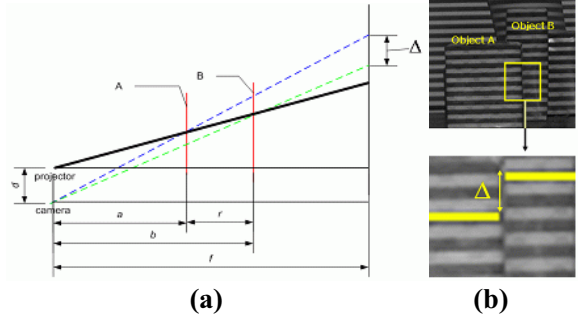


Figure 4. Imaging geometry and the amount of distortion: (a) spatial relation of camera, projector and two object points viewed from the side, Δ : disparity in the image plane of the same horizontal stripe projected onto different object points, (b) the magnitude of pattern distortion, Δ , in a real image

3. Detectable range of depth edges

We have described that we can easily detect depth edges by exploiting the distortion along depth discontinuities in the patterned image. However, as previously mentioned, the distortion may not occur or be sufficient to detect depending the distance of depth edges from the camera or projector. In this section, we present methods to guarantee the occurrence of the distortion for a continuous range of object location.

3.1 Reliably detectable distortion

In order to compute the exact range where depth edges are detectable, we have modeled the imaging geometry of the camera, projector and object as illustrated in Figure 4. The solid line represents a light ray from the projector. When structured light is projected onto object points A and B, they are imaged at different locations in the image plane due to different depth values. That is, distortion of horizontal pattern occurs along the depth discontinuity. The amount of distortion is denoted by Δ . Note that the width of horizontal stripes projected onto object locations A and B are the same in the image plane although they have different depth values. This is because the perspective effect of the camera and projector cancel each other out. From this model, we can derive the following equation using similar triangles.

$$\Delta = fd \left(\frac{1}{a} - \frac{1}{b} \right) = \left(\frac{fdr}{a(a+r)} \right). \quad (4)$$

In order for a depth edge to be detectable by applying a Gabor filter, the disparity of the same horizontal stripe, Δ , in the image plane should be above a certain amount. We have confirmed through

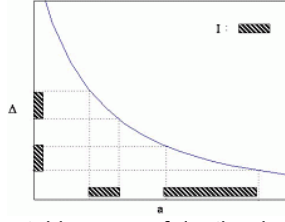


Figure 5. Detectable range of depth edges according to the distance a to object A.

experiments that an offset of at least $2/3$ of the width of the horizontal stripe (w) is necessary for reliable detection of the distortion. Thus, the range of Δ for reliable detection of pattern distortion can be written:

$$2wk + \frac{2w}{3} \leq \Delta \leq 2wk + \frac{4w}{3}, k = 0, 1, \dots \quad (5)$$

From equation (5), given the distance, r , between two object points and the separation, d , between the camera and the projector, we can compute the exact range of the foreground object point, A, from the camera where reliable detection of distortion is guaranteed. Figure 5 depicts the relationship between Δ and a for any k and $k+1$. The marked regions in the horizontal axis, a , represent the ranges of the foreground object point A from the camera that correspond to reliably detectable distortion Δ in the vertical axis. We can see that there are ranges where we cannot detect depth edges due to the lack of distortion depending the distance of a depth edge from the camera or projector. Therefore, for practical application of the proposed approach, we need to guarantee that we are operating within these detectable regions.

3.2 Extending the detectable range of depth edges

We propose two methods to extend the range so that detection of distortion is guaranteed. The first method is based on a single camera and projector setup that uses several structured light images with different width of horizontal stripes. As shown in Figure 6, when we use additional structured light whose spatial period is halved such as $w_2 = 2w_1$, $w_3 = 2w_2$, $w_4 = 2w_3, \dots$, the range of detectable distortion, Δ , is extended. So is the corresponding range, a , of object point location. When n such structured light images are used, the range of detectable distortion, Δ , is expressed as follows.

$$\frac{2}{3}w_1 < \Delta < (2^n - \frac{2}{3})w_1. \quad (6)$$

The second method exploits an additional camera or projector. As illustrated in Figure 7, this method is

equivalent to adding a new curve, $d = d_2$ (the dotted line), that is different from d_1 . Recall that d denotes the distance between the camera and the projector. The new detectable range is created by partially overlapping the ranges by the two curves. A and B represent respectively detectable and undetectable ranges in Δ . They correspond to X and Y regions in a . When $a_1 > a_2$ and $a_4 > a_3$, the undetectable range B in X is overlapped with the detectable range A in Y. Similarly, the undetectable range B in Y is overlapped with the detectable range A in X. Therefore, if we consider both X and Y, we can extend the range where the detection of the distortion is guaranteed. To satisfy the condition $a_1 > a_2$ and $a_4 > a_3$, equation (7) must hold where the range of Δ is $\gamma wk + \alpha w < \Delta < \gamma wk + \beta w, k = 0, 1, \dots$

$$\frac{\alpha + \gamma + \gamma k}{\beta + \gamma k} d_1 < d_2 < \frac{\beta + \gamma k}{\alpha + \gamma k} d_1 \quad (7)$$

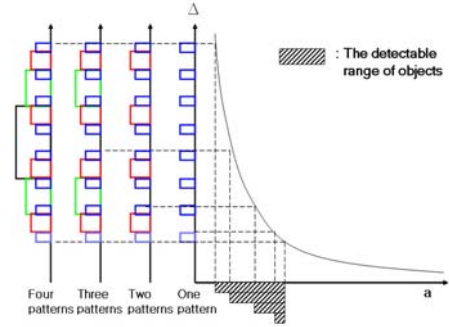


Figure 6. The detectable range of depth edges can be increased by projecting additional structured light with different width of stripes.

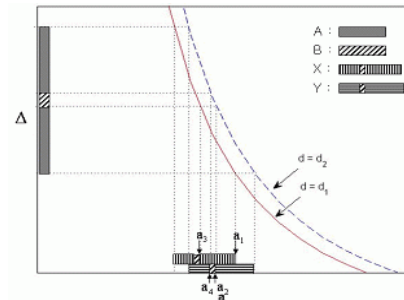


Figure 7. Extending the detectable range using an additional camera or projector

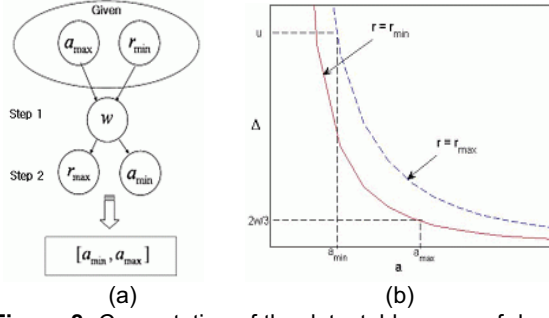


Figure 8. Computation of the detectable range of depth edges: (a) computation process of $[a_{\min}, a_{\max}]$, (b) computation of a_{\min}

3.3 Computation of the detectable range of depth edges

As shown in Figure 8 (a), the detectable range of depth edges $[a_{\min}, a_{\max}]$ is computed in the following two steps:

- (1) Setting the maximum distance of the detectable range, a_{\max} , and the minimum distance between object points, r_{\min} , determines the width of stripes, w , in structured light image.
- (2) This w gives the minimum distance of the detectable range, a_{\min} , resulting in the detectable range of depth edges, $[a_{\min}, a_{\max}]$.

Step 1: Determination of the width of a stripe, w , in the structured light

First, we set a_{\max} to the distance from the camera to the farthest background. Given r_{\min} , w can be computed by equation (8) which is derived from equation (4).

$$w = \frac{3fd_1r_{\min}}{2a_{\max}(a_{\max} + r_{\min})} \quad (8)$$

Thus, given a_{\max} and r_{\min} , we can compute the ideal width of stripes of the structured light. Using this structured light, we can detect depth edges of all object points that are located in the range, $a = [0, a_{\max}]$, and apart from each other no less than r_{\min} .

Step 2: The minimum of the detectable range, a_{\min}

Given w from step 1, we can compute a_{\min} that corresponds to the upper limit of Δ , u , as shown in Figure 8 (b). We have described two methods in section 3.2 for extending the detectable range of depth

edges. The expression for u is different depending on which method is used. Detailed discussion will follow in the next section. After determining u and r_{\max} , a_{\min} can be computed by equation (4). r_{\max} denotes the maximum distance between object points in the range $[a_{\min}, a_{\max}]$ that guarantees the occurrence of the distortion along depth discontinuities. Clearly, the distance between any two object points is bounded by $(a_{\max} - a_{\min})$. Therefore, when a_{\min} and r_{\max} satisfy equation (9), we are guaranteed to detect depth edges of all object points located in the range $[a_{\min}, a_{\max}]$, and apart from each other no less than r_{\min} and no more than r_{\max} .

$$a_{\max} - a_{\min} = r_{\max} \quad (9)$$

In this case, u , a_{\min} and r_{\max} have the following relationship.

$$u = \frac{fd_1r_{\max}}{a_{\min}(a_{\min} + r_{\max})} \quad (10)$$

Then r_{\max} becomes:

$$r_{\max} = \frac{a_{\min}^2 u}{fd_1 - a_{\min} u} \quad (11)$$

Substituting equation (11) into equation (9), we obtain the following equation.

$$a_{\min} = \frac{fd_1 a_{\max}}{fd_1 + u a_{\max}} \quad (12)$$

This way, we can employ structured light of optimal spatial resolution that is most appropriate for given application. Furthermore, we can use this method in an active way to collect information about the scene.

3.4 Detectable range of depth edges

Case 1: a_{\min} based on the first extension method

The upper limit of Δ is $u = (2^n - \frac{2}{3})w_1$ from equation (6). Equating this to u in equation (12) yields a_{\min} as follows:

$$a_{\min} = \frac{fd_1 a_{\max}}{fd_1 + (2^n - \frac{2}{3})a_{\max}} \quad (13)$$

Case 2: a_{\min} based on the second extension method

In order to maximize u that satisfies inequality (7), k must be maximized. Figure 9 plots equation (7) when d_1 is constant. When k has the maximum value, u and a_{\min} can be maximized and minimized,

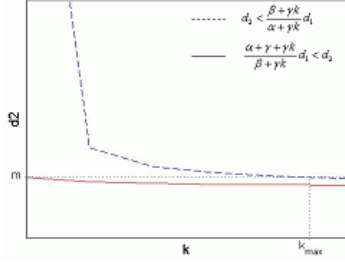


Figure 9. Determination of the distance between camera and projector, d_2

respectively. As shown in Figure 9, at $k = k_{\max}$, d_2 equals m . This gives d_2 as follows:

$$d_2 = \frac{\alpha + \gamma}{\beta} d_1. \quad (14)$$

u is the upper limit value of Δ where $k = \lceil k_{\max} \rceil$. Thus, we obtain

$$u = \beta w_1 + \gamma \lceil k_{\max} \rceil w_1 \quad (15)$$

Substituting equation (15) into equation (12) gives a_{\min} as

$$a_{\min} = \frac{f d a_{\max}}{f d + (\alpha w_1 + \gamma w_1 \lceil k_{\max} \rceil) a_{\max}}. \quad (16)$$

A combined use of the two methods is also possible. In this case, the range of Δ , can be expressed as:

$$\frac{2}{3} w_1 + 2^n w_1 k < \Delta < (2^n - \frac{2}{3}) w_1 + 2^n w_1 k, \quad (17)$$

where, $k = 0, 1, \dots$

Let α, β, γ be

$$\alpha = \frac{2}{3}, \quad \beta = (2^n - \frac{2}{3}), \quad \gamma = 2^n. \quad (18)$$

Substituting α, β, γ into equation (16), we can get a_{\min} when the two extension methods are simultaneously employed.

4. Experimental results

For capturing structured light images, we have used a HP xb31 DLP projector and Canon IXY 500 digital camera. In this section, we present experimental results for two different experimental setups.

A. 1 camera & 1 projector

In order to extend detectable range of depth edges, this setup uses the first method as explained in section 3.2 that just employs additional structured light whose spatial frequency is halved. Figure 10 shows the result of depth edge detection using three structured light

images with different width of horizontal stripes. Figures 16 (a) and (b) display front and side views of the scene, respectively. All the objects are located within the range of 2.4m ~ 3m from the camera. Setting $f = 3\text{m}$, $d = 0.173\text{m}$, $a_{\max} = 3\text{m}$ and $r_{\min} = 0.1\text{m}$,

w_1 and a_{\min} are determined as 0.0084m and 2.325m, respectively. That is, the detectable range of depth edges becomes [2.325m, 3m] and the length of the range is 0.675m. Thus, the widths of stripes of the three structured light that guarantee the detection of depth edges in this range are w_1 , $2w_1$ and $4w_1$.

Figures 10 (c)~(e) show Gabor amplitude maps in the three cases. Each Gabor amplitude map shows that we cannot detect all the depth edges in the scene using a single structured light image. However, combining the results from the three cases, we can obtain the final Gabor amplitude map as in Figure 10 (f) where distortion for detection is guaranteed to appear along depth discontinuities in the range of [2.325m, 3m]. Finally, we can get the depth edge map as in Figure 10 (g). The result shows that this method is capable of detecting depth edges of all the objects located in the detectable range. We have also compared the result with the output of the traditional Canny edge detector (Figure 10 (h)). The proposed method accurately detects depth edges by effectively eliminating inner texture edges of the objects.

B. 1 camera & 2 projector

We can apply both extension methods when using a single camera and two projectors. The detectable range

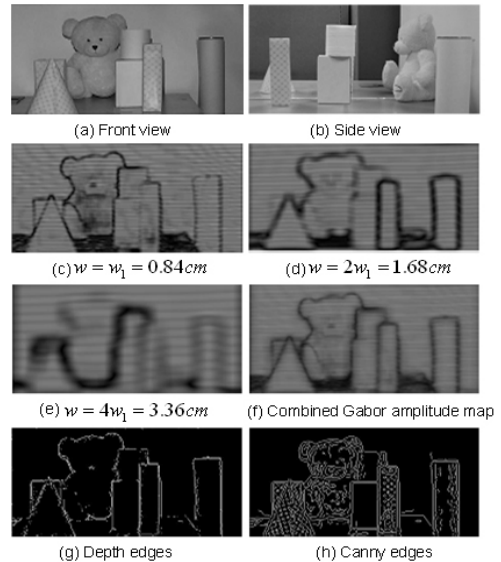


Figure 10: Detecting depth edges using a single camera and projector

can be extended more than setup A when the same number of the structured light images is used. Figure 11 shows the experimental result when two structured lights are used for each projector. Let us call these two projectors as Projector I and Projector II, respectively. The two structured lights are denoted as Structured Light I and Structured Light II. Each projector projects two structured lights. This means that we obtain four patterned images altogether. Figure 11 (a) displays the front view of the scene. All the objects are located within the range of 1.9m~3m from the camera.

When $f=3\text{m}$, $d_1=0.173\text{m}$, $d_2=0.207\text{m}$, $a_{\max}=3\text{m}$, $r_{\min}=0.1\text{m}$ are used, w_1 and a_{\min} are determined as 0.0084m and 1.9375m, respectively. Thus, the detectable range of depth edges becomes [1.9375m, 3m] and the length of the range is 1.0625m. Figures 11 (b)~(e) show how the four structured light images play complementary roles to produce a final depth edge map. While Structured Light I from Projector I cannot detect depth edges between object A and B, Structured Light I from Projector II can. Similarly, the depth edges between object C and D can be detected by Structured Light II from Projector I. These edges cannot be found by Structured Light I from the same projector. Although neither case can detect all the depth edges of the objects, we can get a complete depth edge map by combining the four Gabor amplitude maps. The comparison with the output of the Canny edge detector shows that the proposed method only detects depth edges accurately. Table 1 summarizes pros and cons of experimental setups, A and B, with applications appropriate for each setup. In setup A, not only hardware/software implementation is simple, but also computation is very efficient. It is more suitable to apply to dynamic scenarios such as object and gesture recognition for interactive Human Robot Interface (HRI). Setup B has advantages of wider detectable range and inexpensive computational cost. It is suitable for applications that have relatively less limitation of hardware setup and certain detection range, for example, gesture recognition for human computer interfaces. We are making efforts to achieve the equivalent performance by implementing this setup with a single projector and mirror. Figure 12 (a) shows

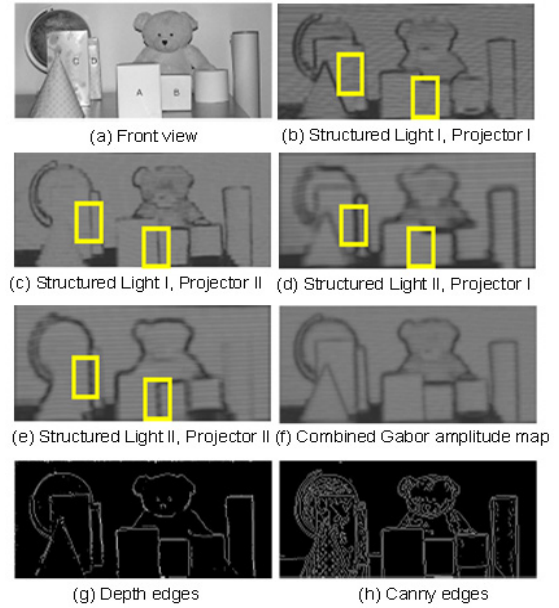


Figure 11: Detecting depth edges using a single camera and two projectors,

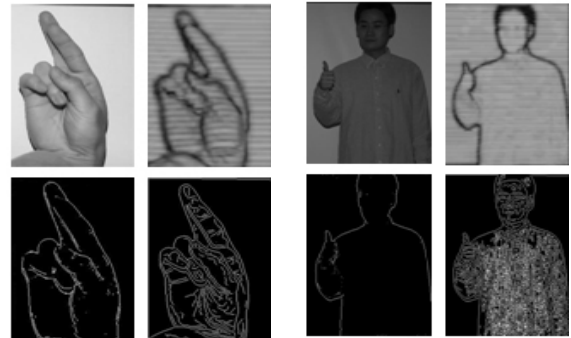


Figure 12: (a) Detection of depth edges in the case of hand gestures for fingerspelling, (b) Detecting human body contours for gesture recognition. Clockwise from top left: white light image, Gabor amplitude map, depth edges and canny edges.

Table 1. Comparison of two experimental setups

	Pros	Cons	Application
setup A: 1 camera& 1 projector	simple and computationally efficient hardware/software setup	less detectable range than that of setup B when the same number of structured lights are used	object recognition for Human Robot Interface
setup B: 1 camera& 2 projector	wider detection range	A small number of structured lights are available when the number of times projection are fixed	gesture recognition

detection of depth edges in the case of hand gestures for fingerspelling. We have only used a single camera and one structured light image to detect hand configuration. We have also applied our method to human body scenes. Figure 12 (b) shows the result of detecting of human body contours. Our method accurately detects depth edges by eliminating inner texture edges by using only a single camera and one structured light image. The result shows that our method is effectively applicable to gesture recognition.

5. Conclusions

We have proposed a new approach using structured light that efficiently computes depth edges. Through a modeled imaging geometry and mathematical analysis, we have also presented three setups that guarantee the occurrence of the distortion along depth discontinuities for a continuous range of object location. These methods enable the proposed approach to be practically applicable to real world scenes. We have demonstrated very promising experimental results.

The setup of one camera and two projectors has advantages of wider distortion range and inexpensive computational cost. We are making efforts to achieve the equivalent performance by implementing it with a single projector and a mirror. In addition, we have observed that infrared projectors show the same distortion characteristics in patterned images. This makes us directly apply the same analysis from the LCD projectors to infrared projectors for the application to Human Robot Interfaces. By bypassing dense 3D reconstruction that is computationally expensive, our methods can be easily extended to dynamic scenes as well. We believe that this research will contribute to great improvement of many computer vision solutions that rely on shape features.

Acknowledgement

This work was supported in part by the Korea Science and Engineering Foundation (KOSEF) through the Biometrics Engineering Research Center (BERC) at Yonsei University.

References

- [1] A. C. Bovik, M. Clark and W. S. Geisler, "Multichannel Texture Analysis Using Localized Spatial Filters," *IEEE Transactions on Pattern Analysis and Machine Intelligence*, pp. 55-73, 1990.
- [2] T. A. Cass, "Robust Affine Structure Matching for 3D Object Recognition," *IEEE Transactions on Pattern Analysis and Machine Intelligence*, pp. 1264-1265, 1998.
- [3] Y. Chen and G. Medioni, "Object Modelling by Registration of Multiple Range Image," *Image and Vision Computing*, pp. 145-155, 1992.
- [4] S. Loncaric, "A survey of shape analysis techniques," *Pattern Recognition*, pp. 983-1001, 1998.
- [5] I. Weiss and M. Ray, "Model-based recognition of 3D object from single vision," *IEEE Transactions on Pattern Analysis and Machine Intelligence*, pp. 116-128, 2001.
- [6] T. Frohlinghaus and J. M. Buhmann "Regularizing phase-based stereo," Proceedings of 13th International Conference on Pattern Recognition, pp. 451-455, 1996.
- [7] W. Hoff and N. Ahuja, "Surfaces from Stereo: Integrating Feature Matching, Disparity Estimation, and Contour Detection," *IEEE Transactions on Pattern Analysis and Machine Intelligence*, Vol. 11, No. 2, pp. 121-136, 1989.
- [8] Sukhan Lee, Jongmoo Choi, Daesik Kim, Byungchan Jung, Jaekeun Na, and Hoonmo Kim, "An Active 3D Robot Camera for Home Environment," Proceedings of 4th IEEE Sensors Conference, 2004.
- [9] D. Scharstein and R. Szeliski, "High-Accuracy Stereo Depth Maps Using Structured Light," IEEE Computer Society Conference on Computer Vision and Pattern Recognition, Vol. 1, pp. 195-202, 2003.
- [10] R. Raskar, K. H. Tan, R. Feris, J. Yu, and M. Turk, "Non-photorealistic Camera: Depth Edge Detection and Stylized Rendering Using Multi-Flash Imaging," Proceedings of ACM SIGGRAPH Conference, Vol. 23, pp. 679-688, 2004.
- [11] R. Feris, M. Turk, R. Raskar, K. Tan, and G. Ohashi, "Exploiting Depth Discontinuities for Vision-based Fingerspelling Recognition," IEEE Workshop on Real-Time Vision for Human-Computer Interaction, 2004.
- [12] W. Ma and B. S. Manjunath, "EdgeFlow: a technique for boundary detection and image segmentation," *IEEE Transactions on Image Processing*, Vol. 9, pp. 1375-1388, 2000.